

# Impact of Covalent Modifications on the Hydrogen Bond Strengths in Diaminotriazine Supramolecules

Andre Nicolai Petelski,<sup>\*[a, b]</sup> Silvana Carina Pamies,<sup>[a]</sup> María Josefina Verónica Márquez,<sup>[a]</sup> Gladis Laura Sosa,<sup>[a, b]</sup> and Nélide María Peruchena<sup>\*[b, c]</sup>

Melamine (M) is a popular triamine triazine compound in the field of supramolecular materials. In this work, we have computationally investigated how substituents can be exploited to improve the binding strength of M supramolecules. Two types of covalent modifications were studied: the substitution of an H atom within an amine group –NHR, and the replacement of the whole –NH<sub>2</sub> group (R=H, F, CH<sub>3</sub> and COCH<sub>3</sub>). Through our dispersion-corrected density functional theory computations, we explain which covalent modification will show the best self-assembling capabilities, and why the binding energy is enhanced. Our charge density and molecular orbital

analyses indicate that the best substituents are those that generate a charge accumulation on the endocyclic N atom, providing an improvement of the electrostatic attraction. At the same time the substituent assists the main N–H...N hydrogen bonds by interacting with the amino group of the other monomer. We also show how the selected group notably boosts the strength of hexameric rosettes. This research, therefore, provides molecular tools for the rational design of emerging materials based on uneven hydrogen-bonded arrangements.

## Introduction

Melamine (M) or 1,3,5-triazine-2,4,6-triamine is a widely used building block in self-assembled supramolecular chemistry<sup>[1]</sup> During the last decades, chemists have been pursuing two of the most craved self-assembled systems: supramolecular polymers<sup>[2,3]</sup> and hydrogen-bonded organic frameworks<sup>[4,5]</sup> (HOF). The former can be obtained by the stacking of cyclic dimers<sup>[6–8]</sup> or hexamers<sup>[9]</sup> of substituted M, while the HOFs are porous materials synthesized by the spontaneous association of M derivatives<sup>[10]</sup> via hydrogen bonds (HBs). The supramolecular diversity of these potential materials is gained through covalent decoration of the diamine triazine moiety.

Melamine is rarely used in its pure form.<sup>[11–13]</sup> Instead, organic chemists have modified M structure in several ways in order to obtain complex supramolecular systems. There are three kinds of modifications. The first one comprises the replacement of a hydrogen atom of an amine group

(–NHR).<sup>[14,15]</sup> This strategy includes –R groups like long alkyl chains with or without rings, the presence of unsaturated sections, and carbonyl groups.<sup>[16]</sup> Chlorine is also used to produced trichloromelamine. This M derivative is commercially used as a sanitizer in food processing establishments.<sup>[17]</sup> Even more, Basu et al.<sup>[18]</sup> have engineered M in such a way to introduce a fluorophore molecule (R<sub>1</sub>) with biological activity and a protein inhibitor (R<sub>2</sub>) within the same amine group of M (–NR<sub>1</sub>R<sub>2</sub>). The second modification consists of the whole replacement of an amine group. For instance, there are reports of substituted M with chlorine,<sup>[19]</sup> methyl<sup>[20]</sup> and aryl<sup>[21,22]</sup> groups. The third approach is the interlocking of two<sup>[23,24]</sup> or three<sup>[25,26]</sup> diamino triazine moieties. The idea of this technique is to pre-organize the assembling and therefore to assist the self-association of a desired structure.

On the other hand, the effects of remote substituents on HBs have been the subject of many theoretical studies. Fonseca Guerra et al. have demonstrated how to tune HBs in guanine-cytosine dimers<sup>[27]</sup> and other Watson–Crick base pairs.<sup>[28]</sup> They have also developed design principles to rationally modulate the HBs in DDAA-AADD (D=donor, A=acceptor, D–H...A) and DAA-ADD dimers.<sup>[29]</sup> Recently, Rodgers et al.,<sup>[30]</sup> have also shown that 5-methylation on protonated cytidine dimers increases its hydrogen bonding energy. Besides, Szatyłowicz et al.<sup>[31]</sup> have analyzed the effects of substituents like NO<sub>2</sub>, Cl, F, H, CH<sub>3</sub>, and NH<sub>2</sub> in three remote positions of adenine and its three cyclic tetramers. In one of their complexes with a nitro group, they have also shown that the presence of side weak interactions can increase the stability of the quartet. Given the vast library of M derivatives in the literature,<sup>[32,33]</sup> one may wonder what the impact of the substituents on the self-assembly of M is if there is any.

In this contribution, we aim to investigate and rationalize the influence of substituents (H, F, CH<sub>3</sub>, and COCH<sub>3</sub>) on M

[a] Dr. A. N. Petelski, S. C. Pamies, M. J. V. Márquez, Prof. Dr. G. L. Sosa  
 Departamento de Ingeniería Química  
 Grupo de Investigación en Química Teórica y Experimental (QUITEX)  
 Universidad Tecnológica Nacional, Facultad Regional Resistencia  
 French 414 (H3500CHJ), Resistencia, Chaco, Argentina  
 E-mail: npetelski@frre.utn.edu.ar

[b] Dr. A. N. Petelski, Prof. Dr. G. L. Sosa, Prof. Dr. N. M. Peruchena  
 Instituto de Química Básica y Aplicada del Nordeste Argentino  
 IQUIBA-NEA, UNNE-CONICET  
 Avenida Libertad 5460, 3400 Corrientes, Argentina  
 E-mail: perunm2014@gmail.com

[c] Prof. Dr. N. M. Peruchena  
 Área de Química Física - Departamento de Química  
 Laboratorio de Estructura Molecular y Propiedades (LEMyP)  
 Facultad de Ciencias Exactas y Naturales y Agrimensura  
 Universidad Nacional del Nordeste  
 Avenida Libertad 5460, 3400 Corrientes, Argentina

Supporting information for this article is available on the WWW under  
<https://doi.org/10.1002/cphc.202200151>

clusters using dispersion-corrected Density Functional Theory (DFT–D). We first analyzed the dimeric forms and then the cyclic and collinear hexamers. Herein, we demonstrate how some substituents can improve the HB energy of M supramolecules, and which one will show the best self-assembling capabilities. This job is of relevance for the design of hydrogen bonding patterns by using diamino triazines as a fundamental building block.

## Computational Details

To analyze the interplay between substituents effects and hydrogen bonding, two types of covalent modifications were chosen, as shown in Figure 1. First, one of the hydrogens of the amine group was fully substituted by fluorine, a methyl group, and a carbonyl group. Then, the whole amine group was substituted by the same groups, including hydrogen (–H, –F, –CH<sub>3</sub>, and –OCH<sub>3</sub>). These modifications are commonly used by experimentalists in the design of M rosettes. All monomers and hydrogen-bonded complexes were then fully optimized with Gaussian 09<sup>[34]</sup> by using the BLYP<sup>[35,36]</sup> functional with the refined version of Grimme dispersion (D3) and the Becke-Johnson<sup>[37]</sup> damping function (BJ). The empirical dispersion correction was implemented with the 3/124=40 IOP keyword. This functional has shown a great performance in M clusters and similar hydrogen-bonded systems.<sup>[38]</sup> The electronic wave function was represented with contracted gaussian-type orbitals<sup>[39]</sup> augmented with diffuse<sup>[40]</sup> and *d* and *p* polarization functions<sup>[41]</sup> by using the split valence 6-311++G(d,p) basis set. The vibrational frequency analysis was used to verify the minimum energy nature of the optimized structures and to compute the Gibbs free energies of bonding.

The interaction energies were computed as the difference between the energy of the supramolecule and the sum of energies of the monomers with the structures they acquire in the complex. The basis set superposition error (BSSE) was corrected using the counterpoise procedure of Boys and Bernardi,<sup>[42]</sup> according to Equation (1):

$$\Delta E_{\text{int}} = E_{\text{AB}} - E_{\text{A}}^{\text{AB}} - E_{\text{B}}^{\text{AB}} \quad (1)$$

where  $E_{\text{AB}}$  is the energy of a general A...B dimer and  $E_{\text{A}}$  and  $E_{\text{B}}$  energies with the superscripts AB are the monomer energies with their dimer-centered basis sets. The interaction energies were then subjected to a localized molecular orbital energy decomposition analysis<sup>[43]</sup> (LMOEDA) at the same level of theory using the

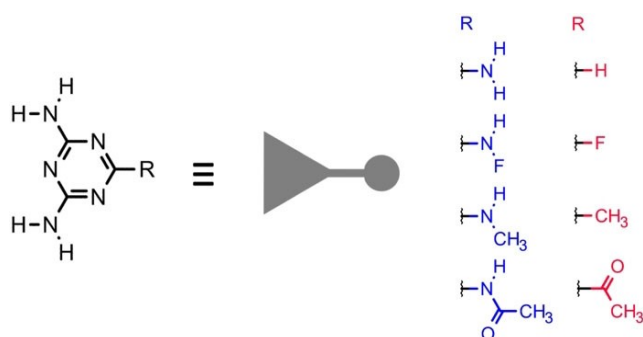


**Figure 1.** Molecular structure of melamine (R=NH<sub>2</sub>) and selected substituent R groups.

GAMESS<sup>[44]</sup> quantum chemistry package. This method partitions the interaction energy into five components, according to Equation (2):

$$\Delta E_{\text{int}} = \Delta E_{\text{ele}} + \Delta E_{\text{ex}} + \Delta E_{\text{rep}} + \Delta E_{\text{pol}} + \Delta E_{\text{disp}} \quad (2)$$

where the term  $\Delta E_{\text{ele}}$  describes the classical electrostatic interaction (Coulombic) of the occupied orbitals of one monomer with those of another monomer;  $\Delta E_{\text{ex}}$  is the attractive exchange component resulting from the Pauli exclusion principle;  $\Delta E_{\text{rep}}$  is the interelectronic repulsion ( $\Delta E_{\text{rep}}$ );  $\Delta E_{\text{pol}}$  accounts for polarization and charge transfer components; and  $\Delta E_{\text{disp}}$  corresponds to the dispersion term.

Secondary interactions were analyzed within two electron density methods. Bond critical points (BCPs) were evaluated within the framework of the quantum theory of atoms in molecules (QTAIM) of Bader,<sup>[45]</sup> and the local properties at the BCPs were computed using the AIMAll<sup>[46]</sup> software. To analyze the nature of the interactions that occur in the different clusters we computed the following topological parameters: The electron charge density  $\rho$  at the BCP; the Laplacian of the electron density  $\nabla^2\rho$  that provides information about the local charge concentration ( $\nabla^2\rho < 0$ ) or depletion ( $\nabla^2\rho > 0$ ) of  $\rho$ ; the total electronic energy density  $H$  that can be associated with the covalent character of a bond when it takes negative values;<sup>[47]</sup> the bond ellipticity  $\epsilon$ , that gives information about the instability of the bond path when it takes high values;<sup>[48]</sup> and finally, the delocalization index  $\delta(\text{A,B})$  that measures the number of electrons delocalized between atoms A and B and it is straight related with the covalent contribution of a bond.<sup>[49,50]</sup> Regions of non-covalent interactions were analyzed with the reduced density gradient<sup>[51]</sup> (RDG) method and computed with the Multiwfn<sup>[52]</sup> program. Molecular electrostatic potential (MEP) surfaces for an isosurface of  $\rho(r)=0.001$  a.u. were computed with AIMAll,<sup>[46]</sup> and  $V_{\text{s,max}}$  and  $V_{\text{s,min}}$  values with Multiwfn software.<sup>[52]</sup> All wave functions were obtained with the hybrid M062X functional of Truhlar and Zhao<sup>[53]</sup> in conjunction with the split valence 6-311++G(d,p) basis using Gaussian 09.<sup>[34]</sup> Orbital interactions were also calculated with the Natural Bond Orbital (NBO) analysis<sup>[54]</sup> as implemented in Gaussian 09.<sup>[34]</sup>

All figures were created with CYLview,<sup>[55]</sup> VMD<sup>[56]</sup> and Marvin.<sup>[57]</sup>

## Results and Discussion

### Structure and Energies of Dimers

When an amine group of M is substituted by an R group, three types of dimers (A, B, and C) can be originated as shown in Figure 2. It has been suggested that the type A dimer is the most favored due to the distance of the bulky groups.<sup>[4]</sup> However, as can be seen in Figure 2a, the so-called secondary electrostatic interactions (SEIs), attractive or repulsive, or substituent effects will code the relative stability of the dimers and finally their binding strengths. Nevertheless, in cases where the substituent is massive, the A-type dimer will probably prevail.<sup>[10]</sup> Depending on the size and length of the substituent, the dimeric forms could generate different types of hydrogen-bonded patterns. For instance, type B could form cyclic hexamers or the so-called rosettes, while type C could form tape-like motifs, as shown in Figure 2b.

We started with the computation of the binding strengths of the three types of dimers. It should be noticed that the

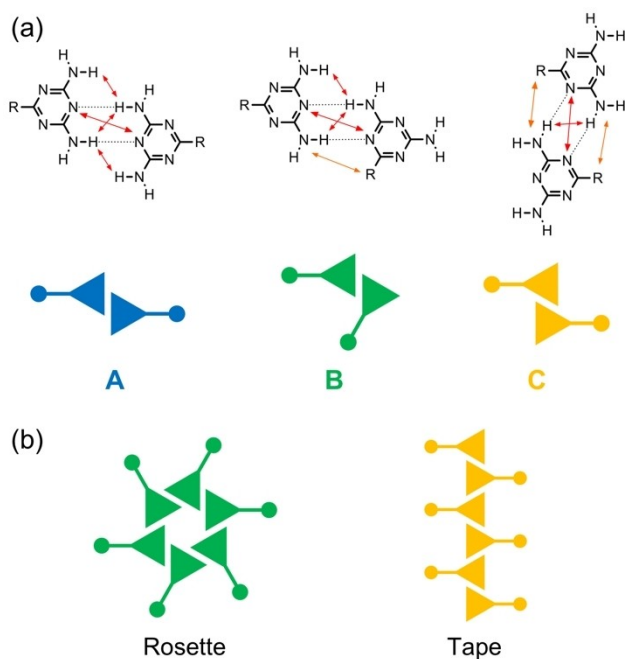


**Figure 2.** a) Dimeric forms of substituted M. Red arrows indicate the repulsive secondary electrostatic interactions (SEIs), and orange arrow indicate SEIs between  $-R$  and  $-NH_2$  groups. b) Type of supramolecular structures.

systems with  $-NHR$  ( $R=H, F, CH_3,$  and  $COCH_3$ ) groups will display different conformers, as shown in Figure 3. This will also be the case of the  $-COCH_3$  group. Therefore, we considered all possible structures.

Figure 4 shows the Gibbs free energies of bonding  $\Delta G_{\text{bond}}$  and the interaction energies  $\Delta E_{\text{int}}$  of the most stable con-

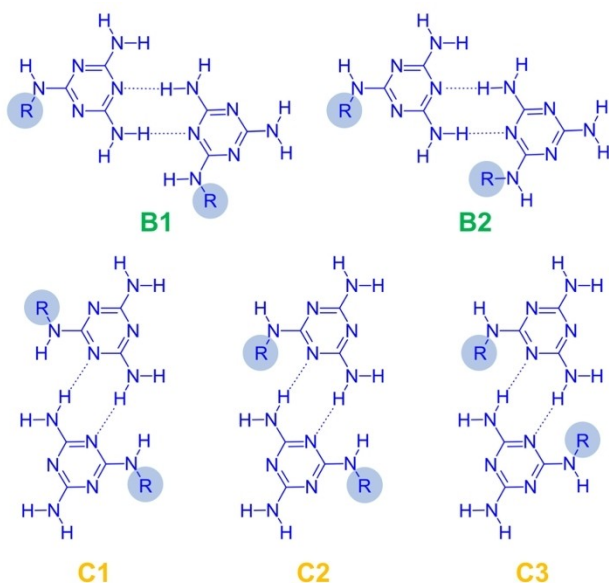


**Figure 3.** Conformers of B and C dimers.

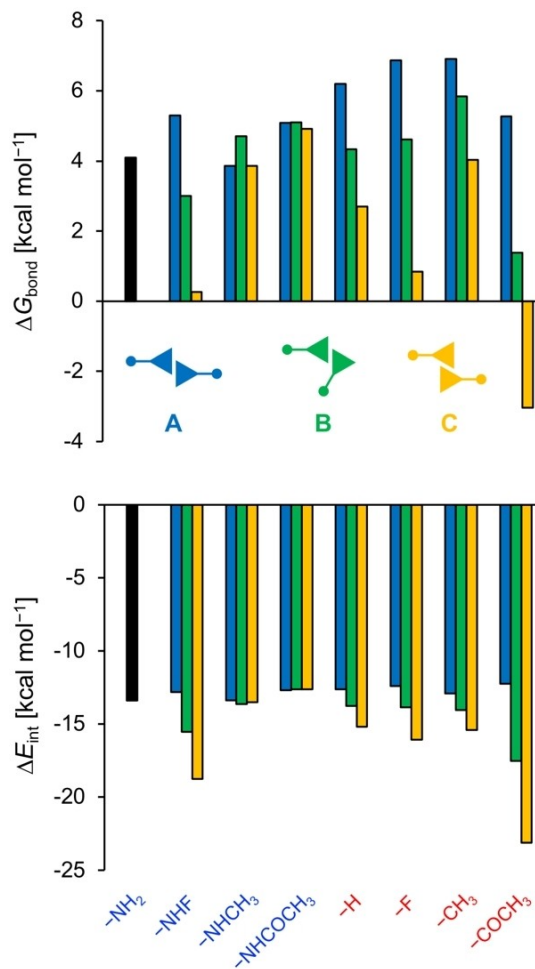


**Figure 4.** Gibbs free energies of bonding and interaction energies of dimers A, B, and C.

formers. This figure clearly shows that the A-type dimer is not the most energetically favored, at least for these simple  $-R$  groups. On the contrary, the most favored dimers are the type C, followed by the Type B. The substituent that produces the most stabilized  $\Delta G_{\text{bond}}$  and  $\Delta E_{\text{int}}$  energies are  $-NHF$  and  $-COCH_3$ . With regards to the other conformers, we found out that type A dimers have the same interaction energy as those of B1 and C1, while B2 dimers have the same energy as C2 dimers (see Table S1 in the Supporting Information). In addition, Figure 4 also shows that all type A dimers show almost the same interaction energies independently of their substituents. As previously demonstrated by Fonseca Guerra et al.,<sup>[29]</sup> the interaction energy of uneven arrangements systems with the same number of HB donor (D) and acceptor (A) atoms cannot be tunable by remote substituents in a predictable way. In systems with DA-AD arrangements, like M dimers, the electronic effects exerted by the remote  $-R$  groups are mutually canceled. Even strong electron-withdrawing groups like  $-CN$  and  $-NO_2$  do not affect so much the interaction energy of a diamine triazine dimer. Type A dimers (see Figure S1) with  $R=CN, NO_2$  gives interaction energies of  $-11.6$  and  $-11.5$  kcal mol<sup>-1</sup>, which

is  $1.8 \text{ kcal mol}^{-1}$  below pure  $M_2$  dimer. Consequently, the main reason that could explain the differences in the interaction energies is the additional interactions between the  $-R$  group of one monomer and the  $-NH_2$  group of the other one.

## Secondary Interactions

Now that we know the relative stability of the dimers, we will identify whether there are secondary interactions between the monomers and the substituents, and how they perturb the main HBs. Since the interaction energy of C1 is equivalent to that of A and B1 dimers, and the interaction energy of C2 is equivalent to that of B2 dimer (see Table S1), we computed the molecular graphs of the C1, C2, and C3 series of dimers for the  $-NHF$  system. We also computed the RDG surfaces and plotted both analyses as shown in Figure 5. Table 1 collects local

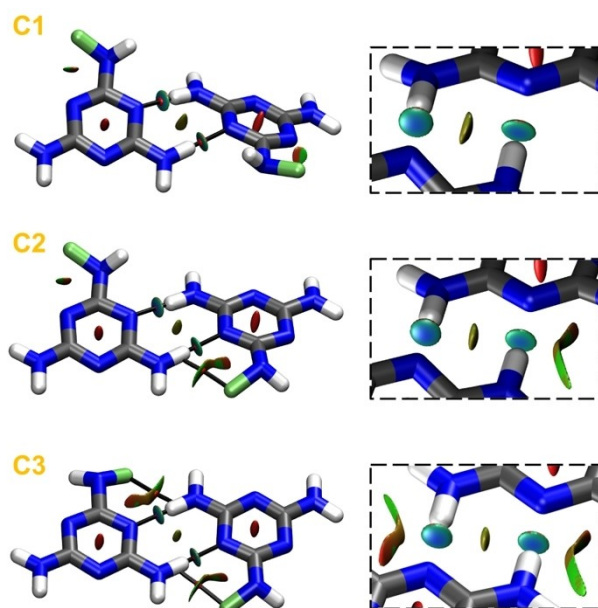


**Figure 5.** Left: Reduce density gradient surfaces superimposed on the molecular graphs of C1, C2 and C3 dimers with  $R = -NHF$ . Right: close-up views of the HBs.

**Table 1.** Local topological parameters (in a.u.) of  $N-H\cdots N$  and  $N-H\cdots F$  interactions for the C1, C2 and C3 dimers with  $R = -NHF$  at  $H\cdots N$  and  $H\cdots F$  BCPs.<sup>[a]</sup>

Conformer	Interaction	$\rho$	$\nabla^2\rho$	H	$\epsilon$	$\delta(H,N/F)$
C1	$N-H\cdots N$	0.028	0.090	0.001	0.070	0.091
	$N-H\cdots N$	0.028	0.090	0.001	0.070	0.091
C2	$N-H\cdots F$	0.008	0.034	0.001	2.417	0.009
	$N-H\cdots N$	0.028	0.090	0.001	0.069	0.085
C3	$N-H\cdots N$	0.030	0.092	0.000	0.071	0.096
	$N-H\cdots F$	0.008	0.036	0.001	1.931	0.008
	$N-H\cdots F$	0.008	0.036	0.001	1.931	0.008
	$N-H\cdots N$	0.030	0.094	0.000	0.069	0.091
	$N-H\cdots N$	0.030	0.094	0.000	0.069	0.091

[a] All values were obtained at B3LYP/6-311 + + G(d,p).

topological values at BCPs. Figure S2 and Table S2 collect the results of the most stabilized system with  $R = COCH_3$ .

As can be seen in Figure 5, C2 and C3 dimers show side interactions between fluorine and the amine group of the opposite monomer. According to the RDG approach, green surfaces are associated with weak attractive interactions. Besides, blue regions are associated with strong attractive interactions.<sup>[51]</sup> Many topological ratios have been defined to classify interactions as closed-shell or shared shell.<sup>[59]</sup> For instance, the ratios  $|V|/G$ <sup>[59]</sup> and  $-G/V$ .<sup>[60]</sup> Since all the BCP show ratios  $|V|/G < 1$  and  $-G/V > 1$  (values not included in Table 1), they can be classified as weak hydrogen bonds (pure closed shell). For weak HBs it is also verified that  $\nabla^2\rho$  and H are positive at the BCP.<sup>[61]</sup> Figure 5 also shows that the H atom of the amine group is involved in a bifurcated HB, this is a BCP between N and H, and between F and the same H. The topological parameters of these interactions (see  $\rho$  and  $\delta(H,N)$  in Table 1) indicate that the  $F\cdots H$  interaction perturbs both  $N-H\cdots N$  HBs. The high ellipticity of the  $F\cdots H$  BCP indicates the instability of this interaction. Within the C2 conformer, one of the  $N-H\cdots N$  HBs experiences an increment of  $\rho$  and  $\delta(H,N)$  with regards to C1, while in C3 both  $N-H\cdots N$  HBs show slightly larger values of  $\rho$  and lower values of H and  $\epsilon$ . In other words, the side interactions are strengthening the  $N-H\cdots N$  HBs. Therefore, type C3 dimers show larger interaction energies than C2 and C1 because of the addition of two side interactions that also improve the main HBs. Besides, the close-up of the C2 dimer (see Figure 5, right side) clearly reveals that one of the HB is stronger than the other one because the RDG surface has a wider blue zone in one of the spots.

## Energy Decomposition Analysis

We can dive more into the nature of the interactions by decomposing the interaction energy of three conformers under the same conditions. To this end, we performed a relaxed scan with the same bond constrains on both  $N-H\cdots N$  interactions within the C1, C2 and C3 dimers with  $R = -NHF$ . We then decomposed the interaction energies at each point and displayed the values in Figure 6 (see full data set in the Supporting Information File). The systems were optimized with  $C_1$  symmetry, and both  $N\cdots N$  distances were varied from 2.7 to 3.0 Å with a 0.02 Å step (15 optimizations).

It is verified that the interaction energy of the C3 conformer is more stabilizing along all the scanned distance. The electrostatic, polarization and dispersion curves follow the same trend of the interaction energy. The three attractive components are more stable for the C3 dimer. These results agree with the analyses of the side interactions. For instance, the first additional  $N-H\cdots F$  interaction will increase the electrostatic attraction between the monomers. This is because when the  $-R$  group includes an electron donating atom, like F in  $-NHF$  or O in  $-COCH_3$ , one of the endocyclic N experiences a larger accumulation of charge. This fact, which is in line with previous observations,<sup>[58]</sup> can be clearly observed in the MEP surfaces and their corresponding  $V_{s,min}$  values as shown in Figure 7. For

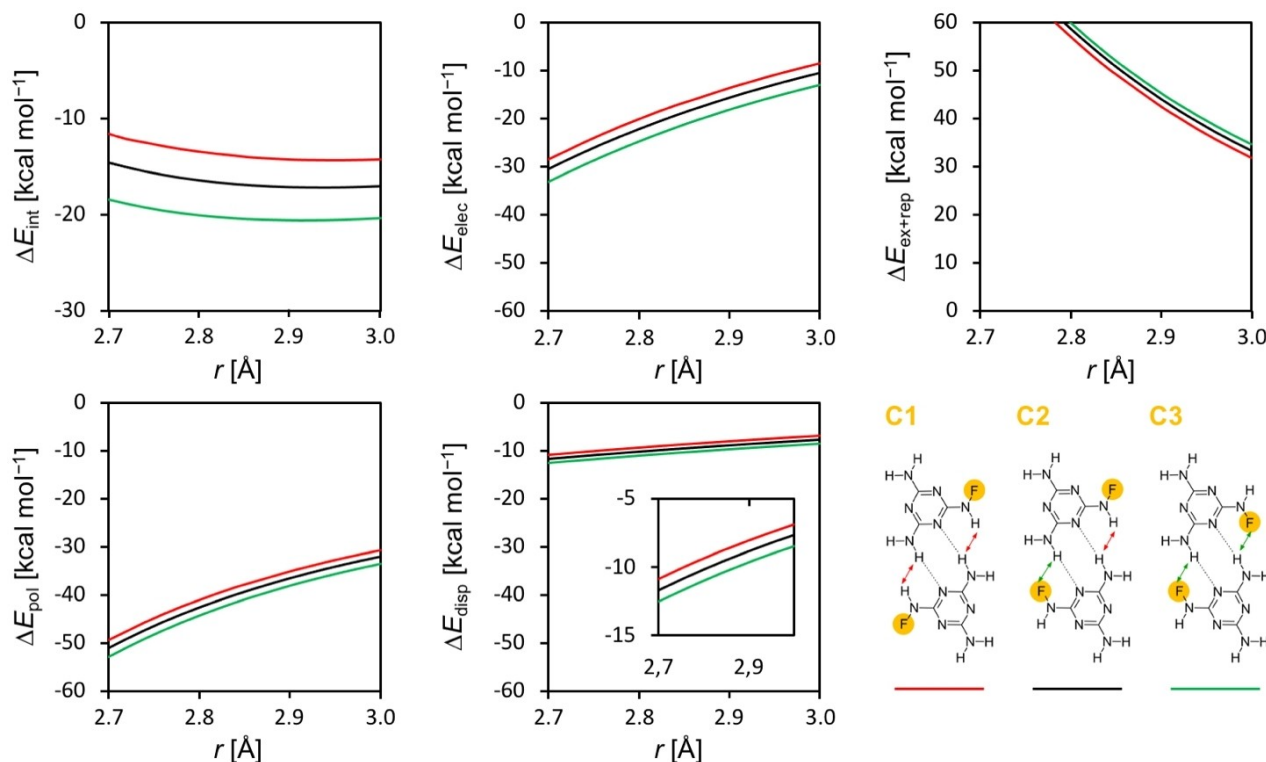


**Figure 6.** Decomposed LMOEDA energy terms [ $\text{kcal mol}^{-1}$ ] as a function of the hydrogen-bond distance  $r$  [ $\text{\AA}$ ] for conformers of type C dimer. The dimers were optimized with constrained linear HBs with distance  $r$  at the BLYP–D3(BJ)/6-311++G(d,p) level of theory.

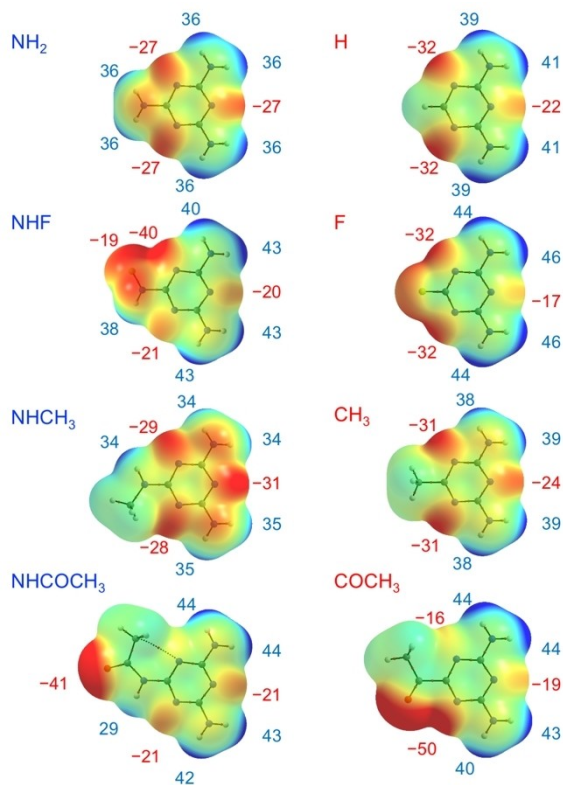


**Figure 7.** Molecular electrostatic potential maps of monomers. The maximum ( $V_{S,\text{max}}$ , blue values) and minimum ( $V_{S,\text{min}}$ , red values) electrostatic potentials (in  $\text{kcal mol}^{-1}$ ) are indicated on the frontier atoms.

example, NHF and COCH<sub>3</sub> systems show the largest charge accumulation on the endocyclic N near the R group:  $-40$  and  $-50 \text{ kcal mol}^{-1}$  respectively. These MEPs also explain why the system with R=H will also show a higher electrostatic attraction between the diamine triazine moieties. The endocyclic N atoms near the H substituent show larger charge accumulation than those of pure M. Therefore, B and C dimers will show a stronger electrostatic attraction, and thus stronger interaction energies than the M<sub>2</sub> dimer. Besides, when analyzing the system with R=NHCOCH<sub>3</sub>, the molecular graph and MEP of Figure 7 explains why the C3 dimer is not more stabilized than the C1 (see also Table S1). The monomer with the NHCOCH<sub>3</sub> substituent is stabilized by an intramolecular BCP between the endocyclic N atom and the  $sp^3$  C atom of the CH<sub>3</sub> group, or the so called tetrel bond.<sup>[62]</sup> This conformer will generate a more stable dimer with a quadruple HB (ADAD-DADA) as shown in Figure S3. To get the C3 dimer with an AD-DA arrangement, the  $-\text{COCH}_3$  group must rotate and therefore break the stabilizing tetrel bond with an energy penalty. Therefore the  $\Delta G_{\text{bond}}$  favors the ADAD-DADA arrangement instead of the AD-DA one. This observation agree with the supramolecules studied by Meijer et al.<sup>[63]</sup>

The side N–H...F interactions also contribute with weak orbital interactions. The second order perturbation energy  $E^{(2)}$  associated to this HB ( $n_{\text{F}} \rightarrow \sigma_{\text{N-H}}^*$ ) is  $0.5 \text{ kcal mol}^{-1}$ . In addition, the energy of the  $n_{\text{N}} \rightarrow \sigma_{\text{N-H}}^*$  charge transfer is  $14.1 \text{ kcal mol}^{-1}$  for both N–H...N interactions within the C1 dimer,  $14.6$  and  $16.9 \text{ kcal mol}^{-1}$  within C2, and  $16.9 \text{ kcal mol}^{-1}$  within C3. There-

fore, the side interactions improve the orbital interaction of the main HBs, as shown in the previous section.

With regards to the repulsion contribution, the C3 dimer shows slightly higher  $\Delta E_{\text{ex+rep}}$  values than C2 and C1. To analyze these differences in Pauli repulsion, we computed the intermolecular overlaps  $S$  between their filled orbitals. When looking this parameter between endocyclic nitrogen lone pairs (HOMO-2) under the same conditions (both distances between N...N), the reported  $S$  value is larger for the C3 dimer, while C1 dimer shows the lowest orbital overlap (see Figure S4 in the supporting Information file). These results agree with the trends in  $\Delta E_{\text{ex+rep}}$  values of Figure 6.

With regards to the repulsion contribution, the C3 dimer shows slightly higher  $\Delta E_{\text{ex+rep}}$  values than C2 and C1. To analyze these differences in Pauli repulsion, we computed the intermolecular overlaps  $S$  between their filled orbitals. When looking this parameter between endocyclic nitrogen lone pairs (HOMO-2) under the same conditions (both distances between N...N), the reported  $S$  value is larger for the C3 dimer, while C1 dimer shows the lowest orbital overlap (see Figure S1 in the supporting Information file). These results agree with the trends in  $\Delta E_{\text{ex+rep}}$  values of Figure 6.

### Structure and Energies of Hexamers

In this section we will test how the secondary interactions operate within larger supramolecules. Hexameric rosettes are one of the most wanted architectures in supramolecular chemistry. Therefore, following our previous analysis on C1, C2 and C3 dimers with -NHF substituents we constructed cyclic and linear hexamers as shown in Figure 8. We also computed the cooperativity effect  $\Delta E_{\text{coop}}$  that occur within the supramolecules according to Equation (3).

$$\Delta E_{\text{coop}} = \Delta E_{\text{int}} - \Delta E_{\text{sum}} \quad (3)$$

Where  $\Delta E_{\text{sum}}$  is the summation of the individual pair interactions as reported previously.<sup>[38]</sup>

If we consider the rotation of the -NHF group, there will be two distinct rosettes as shown in Figures 8a and 8b. The first one is based on the B1 dimer  $^{\text{B1}}(\text{M-NHF})_6$ , while the second one is based on the B2 dimer  $^{\text{B2}}(\text{M-NHF})_6$ . We have shown that the interaction energies of B2 dimers are more stabilizing than the B1 dimers, and this trend also prevails within the rosettes. The  $^{\text{B2}}(\text{M-NHF})_6$  hexamer has an interaction energy  $19.2 \text{ kcal mol}^{-1}$  larger than the  $^{\text{B1}}(\text{M-NHF})_6$  conformer. In addition, both rosettes have the same cooperativity effect. This means that one of the N-H...N HBs is stronger than the other one, as was demonstrated by the computed local topological parameters. Furthermore, an hexameric rosette of pure M, this is  $(\text{M-NH}_2)_6$ , has the same interaction energy as that of  $^{\text{B1}}(\text{M-NHF})_6$ . Therefore, the electronic effect exerted by the F atom is cancelled due to the DA-AD arrangement of the HBs. Thus, in these cases, the supramolecular binding strength can only be tuned by secondary interactions.

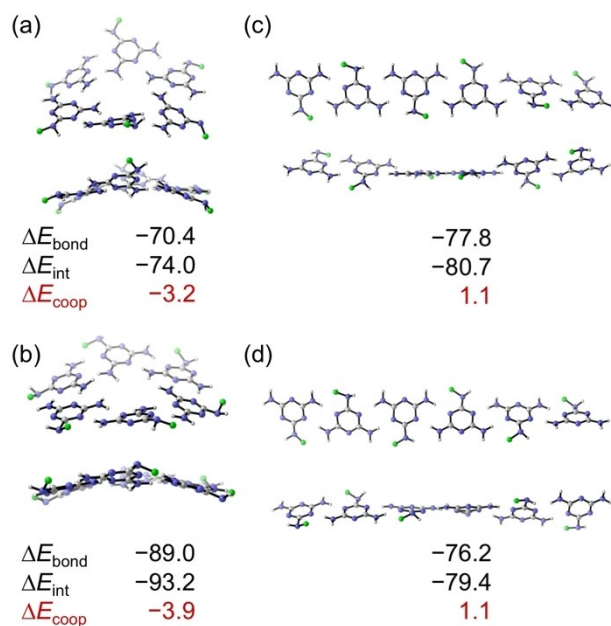


**Figure 8.** Top and side structures of cyclic and linear hexamers with R=NHF. Energies are in kcal mol<sup>-1</sup>. a)  $^{\text{B1}}(\text{M-NHF})_6$  rosette, b)  $^{\text{B2}}(\text{M-NHF})_6$  rosette, c) C3-C1-C3-C1-C3 linear hexamer, and d) C3-C2-C2-C2-C2 linear hexamer.

When analyzing the linear hexamers, there can be many conformers because of the rotation of the NHF group. Here in we analyzed only two combinations of dimers. Figure 8c shows a combination of C3-C1-C3-C1-C3 dimers, and Figure 8d shows a colinear arrangement of C3-C2-C2-C2-C2 dimers. Both conformers display almost the same interaction and bonding energies, and they do not develop a positive cooperativity. Thus, it is easy to think that any other arrangement will have the same interaction energy. Lastly, the  $^{\text{B1}}(\text{M-NHF})_6$  cyclic hexamer is around  $7 \text{ kcal mol}^{-1}$  more stable than both linear hexamers, while the  $^{\text{B2}}(\text{M-NHF})_6$  rosette is more stabilized by around  $12 \text{ kcal mol}^{-1}$ . For this reason, the secondary interactions not only improve the interaction energy of the dimers, but also increase the difference in stability between cyclic and linear hexamers, favoring thus the self-assembling of rosettes.

### Conclusions

In conclusion, we have analyzed the impact of two types of substituents on the supramolecular self-assembly of melamine derivatives. Through our quantum chemical computations, we have provided a fundamental basis to rationally improve the binding strength of diaminotriazines through covalent decoration. We assessed the performance of the interactions with different charge density and molecular orbital analyses.

Our results demonstrate that the best substituent group are those that generate a larger charge accumulation within the endocyclic nitrogen near the R group. This effect will therefore increase the electrostatic attraction between the monomers.

Since the remote substituent effects are mutually cancelled within DA-AD arrangements, the R group must also interact with the  $-NH_2$  group of the other monomer via hydrogen-bonding. This secondary interaction increases the electrostatic attraction and contributes with weak orbital interactions. The substituents that fulfill these requirements are the methyl ketone group ( $-COCH_3$ ) followed by the  $-NHF$  group.

Finally, our results indicate that secondary interactions can be used as a tool not only to improve the dimerization energy between diamino triazine moieties, but also to improve the stability of cyclic hexamers and tune other uneven hydrogen-bonded arrays.

## Acknowledgements

The authors gratefully acknowledge the financial support from the Secretaría de Ciencia y Tecnología, Universidad Tecnológica Nacional, Facultad Regional Resistencia (SCYT-UTN-FRRe). M. J. V. M. thanks the SCYT-UTN-FRRe for a Research and Development Initiation Scholarship. A. N. P. and N. M. P. are CONICET career researchers.

## Conflict of Interest

The authors declare no conflict of interest.

## Data Availability Statement

The data that support the findings of this study are available in the supplementary material of this article.

**Keywords:** amines · hydrogen bonds · self-assembly · substituent effects · isomers

- [1] B. Roy, P. Baire, A. K. Nandi, *RSC Adv.* **2014**, *4*, 1708.
- [2] J.-M. Lehn, *Proc. Natl. Acad. Sci. USA* **2002**, *99*, 4763–4768.
- [3] T. Aida, E. W. Meijer, S. I. Stupp, *Science* **2012**, *335*, 813–817.
- [4] Y.-F. Han, Y.-X. Yuan, H.-B. Wang, *Molecules* **2017**, *22*, 266.
- [5] J. Luo, Wang, J. W. J. H. Zhang, S. Lai, D. C. Zhong, *CrystEngComm* **2018**, *20*, 5884–5898.
- [6] A. P. H. J. Schenning, P. Jonkheijm, F. J. M. Hoebe, J. van Herrikuhyzen, S. C. J. Meskers, E. W. Meijer, L. M. Herz, C. Daniel, C. Silva, R. T. Phillips, R. H. Friend, D. Beljonne, A. Miura, S. De Feyter, M. Zdanowska, H. Uji-i, F. C. De Schryver, Z. Chen, F. Würthner, M. Mas-Torrent, D. den Boer, M. Durkut, P. Hadley, *Synth. Met.* **2004**, *147*, 43–48.
- [7] T. Seki, S. Yagai, T. Karatsu, A. Kitamura, *J. Org. Chem.* **2008**, *73*, 3328–3335.
- [8] J. H. K. K. Hirschberg, L. Brunsveid, A. Ramzi, J. A. J. M. Vekemans, R. P. Sijbesma, E. W. Meijer, *Nature* **2000**, *407*, 167–170.
- [9] B. Adhikari, X. Lin, M. Yamauchi, H. Ouchi, K. Aratsu, S. Yagai, *Chem. Commun.* **2017**, *53*, 9663–9683.
- [10] H. Sauriat-Dorizon, D. Laliberté, T. Maris, J. D. Wuest, *J. Org. Chem.* **2003**, *68*, 240–246.
- [11] H. Zhang, Z. Xie, L. Long, H. Zhong, W. Zhao, B.-W. Mao, X. Xu, L.-S. Zheng, *J. Phys. Chem. C* **2008**, *111*, 4209–4218.
- [12] A. Ciesielski, S. Haar, G. Paragi, Z. Kupihár, Z. Kele, S. Masiero, C. Fonseca Guerra, F. M. Bickelhaupt, G. P. Spada, L. Kovács, P. Samorí, *Phys. Chem. Chem. Phys.* **2013**, *15*, 12442.
- [13] J. Zhang, Y. Feng, R. J. Staples, J. Zhang, J. M. Shreeve, *Nat. Commun.* **2021**, *12*, 4–10.
- [14] A. G. Bielejewska, C. E. Marjo, L. J. Prins, Timmerman, P. F. de Jong, D. N. Reinhoudt, *J. Am. Chem. Soc.* **2001**, *123*, 7518–7533.
- [15] M. List, H. Puchinger, H. Gabriel, U. Monkowius, C. Schwarzinger, *J. Org. Chem.* **2016**, *81*, 4066–4075.
- [16] B. J. Cafferty, I. Gállego, M. C. Chen, K. I. Farley, R. Eritja, N. V. Hud, *J. Am. Chem. Soc.* **2013**, *135*, 2447–2450.
- [17] WORLD HEALTH ORGANIZATION, Toxicological and health aspects of melamine and cyanuric acid: report of a WHO expert meeting in collaboration with FAO, supported by Health Canada, Ottawa, Canada, 1–4 December 2008. 2009.
- [18] C. Ghosh, A. Nandi, S. Basu, *Nanoscale* **2019**, *11*, 3326–3335.
- [19] T. Le, M. Bhadbhade, J. Gao, J. M. Hook, C. E. Marjo, *CrystEngComm* **2016**, *18*, 962–970.
- [20] A. Delori, E. Suresh, V. R. Pedireddi, *Chem. Eur. J.* **2008**, *14*, 6967–6977.
- [21] P. Jonkheijm, A. Miura, M. Zdanowska, F. J. M. Hoebe, S. De Feyter, A. P. H. J. Schenning, F. C. De Schryver, E. W. Meijer, *Angew. Chem. Int. Ed. Engl.* **2004**, *43*, 74–78.
- [22] K. E. Maly, C. Dauphin, J. D. Wuest, *J. Mater. Chem.* **2006**, *16*, 4695.
- [23] I. S. Choi, X. Li, E. E. Simanek, R. Akaba, G. M. Whitesides, *Chem. Mater.* **1999**, *11*, 684–690.
- [24] J. M. C. A. Kerckhoffs, M. G. J. ten Cate, M. A. Mateos-Timoneda, F. W. B. van Leeuwen, B. Snellink-Ruël, A. L. Spek, H. Kooijman, M. Crego-Calama, D. N. Reinhoudt, *J. Am. Chem. Soc.* **2005**, *127*, 12697–12708.
- [25] C. T. Seto, G. M. Whitesides, *J. Am. Chem. Soc.* **1993**, *115*, 905–916.
- [26] M. Ma, D. Bong, *Langmuir* **2011**, *27*, 8841–8853.
- [27] C. Fonseca Guerra, Z. Szekeres, F. M. Bickelhaupt, *Chem. Eur. J.* **2011**, *17*, 8816–8818.
- [28] C. Fonseca Guerra, T. van der Wijst, F. M. Bickelhaupt, *Struct. Chem.* **2005**, *16*, 211–221.
- [29] S. C. C. Van Der Lubbe, A. Haim, T. Van Heesch, C. Fonseca Guerra, *J. Phys. Chem. A* **2020**, *124*, 9451–9463.
- [30] Y. S. Seidu, H. A. Roy, M. T. Rodgers, *J. Phys. Chem. A* **2021**, *125*, 5939–5955.
- [31] H. Szatyłowicz, P. H. Marek, O. A. Stasyuk, T. M. Krygowski, M. Solà, *RSC Adv.* **2020**, *10*, 23350–23358.
- [32] B. Bann, S. A. Miller, *Chem. Rev.* **1958**, *58*, 131–172.
- [33] J. R. Campbell, R. E. Hatton, *J. Org. Chem.* **1959**, *26*, 2786–2789.
- [34] Gaussian 09, Revision D.01, M. J. Frisch, G. W. Trucks, H. B. Schlegel, G. E. Scuseria, M. A. Robb, J. R. Cheeseman, G. Scalmani, V. Barone, B. Mennucci, G. A. Petersson, H. Nakatsuji, M. Caricato, X. Li, H. P. Hratchian, A. F. Izmaylov, J. Bloino, G. Zheng, J. L. Sonnenberg, M. Hada, M. Ehara, K. Toyota, R. Fukuda, J. Hasegawa, M. Ishida, T. Nakajima, Y. Honda, O. Kitao, H. Nakai, T. Vreven, J. A. Montgomery, Jr., J. E. Peralta, F. Ogliaro, M. Bearpark, J. J. Heyd, E. Brothers, K. N. Kudin, V. N. Staroverov, T. Keith, R. Kobayashi, J. Normand, K. Raghavachari, A. Rendell, J. C. Burant, S. S. Iyengar, J. Tomasi, M. Cossi, N. Rega, J. M. Millam, M. Klene, J. E. Knox, J. B. Cross, V. Bakken, C. Adamo, J. Jaramillo, R. Gomperts, R. E. Stratmann, O. Yazyev, A. J. Austin, R. Cammi, C. Pomelli, J. W. Ochterski, R. L. Martin, K. Morokuma, V. G. Zakrzewski, G. A. Voth, P. Salvador, J. J. Dannenberg, S. Dapprich, A. D. Daniels, O. Farkas, J. B. Foresman, J. V. Ortiz, J. Cioslowski, D. J. Fox, Gaussian, Inc., Wallingford CT, 2013.
- [35] A. D. Becke, *Phys. Rev. A* **1988**, *38*, 3098–3100.
- [36] C. Lee, W. Yang, R. G. Parr, *Phys. Rev. B* **1988**, *37*, 785–789.
- [37] S. Grimme, *J. Comput. Chem.* **2004**, *25*, 1463–1473.
- [38] A. N. Petelski, C. Fonseca Guerra, *ChemistryOpen* **2019**, *8*, 135–142.
- [39] A. D. McLean, G. S. Chandler, *J. Chem. Phys.* **1980**, *72*, 5639–5648.
- [40] T. Clark, J. Chandrasekhar, G. W. Spitznagel, P. V. R. Schleyer, *J. Comput. Chem.* **1983**, *4*, 294–301.
- [41] M. J. Frisch, J. A. Pople, J. S. Binkley, *J. Chem. Phys.* **1984**, *80*, 3265–3269.
- [42] S. F. Boys, F. Bernardi, *Mol. Phys.* **1970**, *19*, 553–559.
- [43] P. Su, H. Li, *J. Chem. Phys.* **2009**, *131*, 014102.
- [44] M. W. Schmidt, K. K. Baldridge, J. A. Boatz, S. T. Elbert, M. S. Gordon, J. H. Jensen, S. Koseki, N. Matsunaga, K. A. Nguyen, S. Su, T. L. Windus, M. Dupuis, J. A. Montgomery, *J. Comput. Chem.* **1993**, *14*, 1347–1363.
- [45] R. F. W. Bader, *Atoms in Molecules: A Quantum Theory*, Clarendon Press: Oxford, **1994**.
- [46] T. A. Keith, AIMAll (Version 11.12.19); TK Gristmill Software, Overland Park KS; Aim.Tkgristmill.Com. TK Gristmill Software: Overland Park KS 2011.
- [47] S. Nanayakkara, E. Kraka, *Phys. Chem. Chem. Phys.* **2019**, *21*, 15007–15018.
- [48] P. L. A. Popelier, *J. Phys. Chem. A* **1998**, *102*, 1873–1878.

- [49] C. Outeiral, M. A. Vincent, Á. Martín Pendás, P. L. A. Popelier, *Chem. Sci.* **2018**, *9*, 5517–5529.
- [50] A. M. Pendás, J. L. Casals-Sainz, E. Francisco, *Chem. Eur. J.* **2019**, *25*, 309–314.
- [51] E. R. Johnson, S. Keinan, P. Mori-Sánchez, J. Contreras-García, A. J. Cohen, W. Yang, *J. Am. Chem. Soc.* **2010**, *132*, 6498–6506.
- [52] T. Lu, F. Chen, *J. Comb. Chem.* **2012**, *33*, 580–592.
- [53] Y. Zhao, D. G. Truhlar, *Theor. Chem. Acc.* **2008**, *120*, 215–241.
- [54] a) A. E. Reed, L. A. Curtiss, F. Weinhold, *Chem. Rev.* **1988**, *88*, 899–926; b) E. D. Glendening, J. K. Badenhoop, A. E. Reed, J. E. Carpenter, F. Weinhold, NBO Version 3.1; Theoretical Chemistry Institute, University of Wisconsin: Madison, WI.
- [55] CYLview, 1.0b; C. Y., Legault, Université de Sherbrooke, 2009 (<http://www.Cylview.Org>).
- [56] W. Humphrey, A. Dalke, K. Schulten, *J. Mol. Graphics* **1996**, *14*, 33–38.
- [57] Marvin 19.13.0, 2019, ChemAxon (<http://www.Chemaxon.Com>).
- [58] S. C. C. Van Der Lubbe, F. Zaccaria, X. Sun, C. Fonseca Guerra, *J. Am. Chem. Soc.* **2019**, *141*, 4878–4885.
- [59] I. Mata, I. Alkorta, E. Espinosa, E. Molins, J. Elguero, in *The Quantum Theory of Atoms in Molecules. From Solid State to DNA and Drug Design* (Eds.: C. F. Matta, R. J. Boyd), Wiley-VCH, Weinheim, **2007**, pp. 425–451.
- [60] R. P. Orenha, N. H. Morgon, J. Contreras-García, G. Cappato Guerra Silva, G. R. Nagurniak, M. J. Piotrowski, G. F. Caramori, A. Muñoz-Castro, R. L. T. Parreira, *New J. Chem.* **2020**, *44*, 773–779.
- [61] E. Espinosa, I. Alkorta, J. Elguero, E. Molins, *J. Chem. Phys.* **2002**, *117*, 5529–5542.
- [62] S. Scheiner, *Phys. Chem. Chem. Phys.* **2021**, *23*, 5702–5717.
- [63] F. H. Beijer, H. Kooijman, A. L. Spek, R. P. Sijbesma, E. W. Meijer, *Angew. Chem. Int. Ed. Engl.* **1998**, *37*, 75–78.

---

Manuscript received: March 7, 2022  
Revised manuscript received: April 13, 2022  
Accepted manuscript online: April 14, 2022  
Version of record online: May 13, 2022